

## Regular article

# The occurrence of electron transfer in aromatic nitration: dynamical aspects

Alexandra Romina Albuñia<sup>1</sup>, Raffaele Borrelli<sup>2</sup>, Andrea Peluso<sup>1</sup>

<sup>1</sup>Dipartimento di Chimica, Università di Salerno, 84081 Baronissi, Salerno, Italy

<sup>2</sup>Cattedra di Chimica Teorica, Università Federico II, via Mezzocannone 4, 80134 Naples, Italy

Received: 16 September 1999 / Accepted: 3 February 2000 / Published online: 12 May 2000

© Springer-Verlag 2000

**Abstract.** Electron transfer (ET) from toluene to the nitronium ion in the region of van der Waals intermolecular distances has been investigated by a quantum dynamical analysis performed on potential-energy surfaces computed at the *ab initio* multireference configuration interaction level. The results show that ET is very fast, occurring on a timescale of a few picoseconds. This has important implications for the mechanism of aromatic nitration: the ET path can compete efficiently with the direct attack of the nitronium ion to the aromatic substrate to yield the Wheland intermediate and that could explain some unsettled points in the mechanism of aromatic nitration.

**Key words:** Aromatic nitration – Electron transfer – Quantum dynamics

## 1 Introduction

The pioneering work of Ingold's group on aromatic nitration represents a cornerstone in the development of mechanistic models of organic reactions [1]; however, in Ingold's mechanism there were still unsettled points. The main matter of debate concerns the clear-cut selectivity toward the substitution position, even though the reaction rate is nearly encounter-limited [2]. In simple words, it is difficult to understand why the meta carbons of toluene are not nitrated, even though toluene and benzene react at nearly the same rate. Olah was the first to make this objection and suggested as a possible explanation that the attack of the nitronium ion to the aromatic substrate occurs in two steps. The first step, which is the rate-determining one, consists of the formation of a  $\pi$  complex between the reactants and is responsible for substrate selectivity; the second step, which should be faster, leads to the Wheland intermediate and accounts for positional selectivity. Further evidence in favor of the two-step mechanism has been

provided by Ridd [3], who has shown that the changes in the kinetics expression on varying the reaction conditions can be well explained only by a two-step mechanism.

Although Olah's two-step mechanism formally accounts for the above difficulty, because the rate of formation of the Wheland intermediate is now different from the rate of the attack of the nitronium ion to the aromatic substrate, it is still difficult to see how the formation of a  $\pi$  complex can account for the observed positional selectivity. Therefore, Perrin [4] proposed a different two-step mechanism, consisting of an electron-transfer (ET) step from the aromatic substrate to  $\text{NO}_2^+$ , followed by a fast radical recombination to give the Wheland intermediate. Perrin claimed that an ET step would solve the problem posed by the consideration that if the attacking species were  $\text{NO}_2^+$  there should be no positional selectivity. In fact, in the ET mechanism the attacking species is the  $\text{NO}_2$  radical and the selectivity toward the substitution position can be ascribed to the very different spin density at the substrate carbons.

The occurrence of an ET step in aromatic nitration had been proposed several times, on the grounds of a relationship between the substitution rates and the ionization potentials of the substrates [5], but it never enjoyed much success and was rejected by Ingold's group because the addition of  $\text{NO}_2$  to the reactants gives products which are not found in the normal reaction [6]. Even the experimental and theoretical evidence provided by Perrin have been criticized: the main argument against the ET path was that, if the conditions implicit in Marcus's theory apply, then the transfer of an electron from an aromatic ring to the nitronium ion should be a slow process characterized by a high potential-energy barrier. Using molecular mechanics, a barrier of 52 kcal/mol for the outer sphere ET process has been estimated [7].

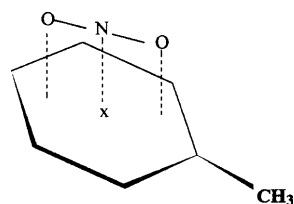
Recently, the possibility of an inner-sphere ET process has been considered. The analysis of the potential-energy surfaces of the lowest-energy singlet states of the van der Waals toluene- $\text{NO}_2^+$  complex in the gas phase suggested that both the formation of a  $\pi$  complex and its evolution in a contact radical pair (ET) are thermodynamically plausible steps [8]. The potential-energy

barrier for ET was estimated to be about 12 kcal/mol at *ab initio* multireference configuration interaction (MRCI)/3-21G level. Although the barrier to ET is now much lower than previous estimates, the involvement of an ET step in the mechanism of aromatic nitration is still questionable. In fact, *ab initio* Hartree–Fock (HF)/fourth-order Møller–Plesset perturbation/3-21G computations predict that the direct attack of the nitronium ion to the aromatic substrate occurs without an energy barrier, both for benzene and for toluene [9]. This result is indeed very puzzling, because on one hand, it would indicate that the one-step mechanism is the preferred path, but, on the other hand, it is evident that this cannot account for the clear-cut positional selectivity of aromatic nitration. At any rate, the possibility that the ET step would be fast, thus competing with the direct attack of the nitronium ion to the aromatic ring, is not ruled out by the computations and is therefore worthy of further investigation.

In this article we consider the dynamical aspects of the ET step by determining the transition probabilities as a function of the time for the electron donor–acceptor  $\pi$  complex to evolve in a contact radical pair. We show that in the case of the toluene substrate ET occurs on a timescale of a few picoseconds, thus making the ET path very probable.

## 2 Results

Let us start by considering that the nitronium ion has formed a  $\pi$  complex with the toluene substrate. In the region of intermolecular van der Waals distances, where electrostatic forces predominate, it is expected that the  $\text{NO}_2^+$  axis is parallel to the aromatic plane, with the nitrogen atom, which carries all the positive charge, located approximately above the center of the aromatic ring as shown in Scheme 1.



Scheme 1

If ET from toluene to  $\text{NO}_2^+$  occurs, then it would mainly involve the stretching and the bending coordinate of  $\text{NO}_2^+$ . In fact, the geometry of the toluene radical cation is not significantly different from that of the neutral molecule, whereas the geometry of the linear  $\text{NO}_2^+$  differs significantly from that of the neutral radical, which is bent, with a valence angle of  $136^\circ$ , and which has a slightly longer N–O bond length (1.19 versus 1.11 Å). Thus, it is sufficient to consider the time evolution over the two-dimensional projection of the potential-energy hypersurfaces obtained by allowing the symmetrical stretching,  $\Delta R = 1/\sqrt{2}(\Delta r_1 + \Delta r_2)$ , and the bending,  $\Delta\Theta$ , coordinates of  $\text{NO}_2^+$  to move and keeping all other

coordinates fixed to the value corresponding to the equilibrium point of the initial  $\pi$  complex. The optimized geometry of toluene (restricted HF/6-31G) was used throughout the computations. As concerns the mutual orientation of the two moieties in the initial complex, we considered that shown in Scheme 1, which is probably not the most favorable to ET [8], but would better represent the random formation of an encounter pair.

### 2.1 Adiabatic states

The energies and shapes of the adiabatic states of the [toluene– $\text{NO}_2^+$ ] pair were evaluated using the MRCI technique, using the Gamess package [10] and the standard 6-31G basis set. The active space includes the two highest filled  $\pi$  levels of toluene, the three lowest empty  $\pi$  levels of  $\text{NO}_2^+$  and the two lowest empty  $\pi$  levels of toluene. Furthermore all the single excited configurations arising from promoting an electron from any level of the active space to one of the lowest 21 virtual orbitals were considered.

The potential-energy map for the adiabatic ET from toluene to  $\text{NO}_2^+$ , as a function of the bending and symmetric stretching coordinate of  $\text{NO}_2^+$ , is reported in Fig. 1. The minimum associated with the reactants ( $\Theta = 175^\circ$ ,  $r_1 = r_2 = 1.11$  Å) lies about 1 eV above that of the ET products ( $\Theta = 132^\circ$ ,  $r = 1.21$  Å; the barrier for adiabatic ET is about 4 kcal/mol. For  $\Theta$  in the range  $180^\circ$ – $150^\circ$ , the lowest adiabatic state is mainly given by the ground-state configuration, with the positive charge localized on the nitronium ion ( $|\text{ArHNO}_2^+\rangle$ ) whereas for smaller values of  $\Theta$ , the lowest adiabatic state mainly corresponds to a singly excited configuration, obtained by promoting an electron from the highest occupied

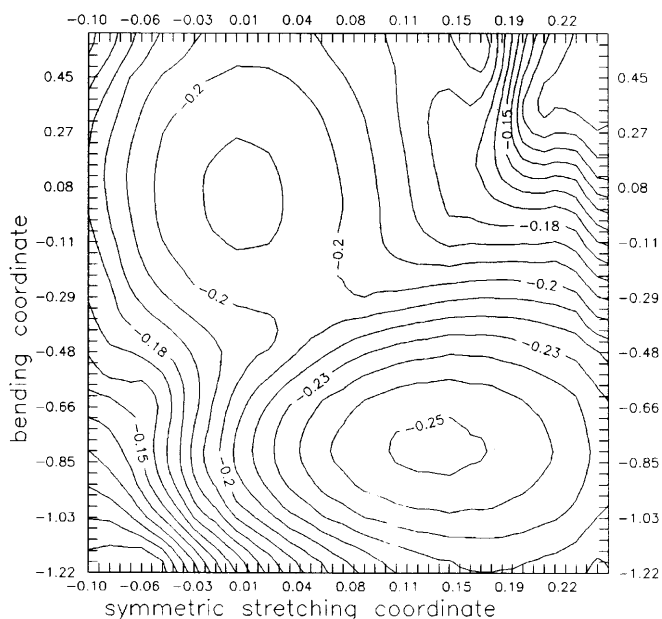


Fig. 1. Potential-energy map for adiabatic electron transfer (ET) from toluene to  $\text{NO}_2^+$  as a function of the bending ( $r\Delta\Theta$  in angstroms) and symmetric stretching coordinate of  $\text{NO}_2^+$  (Å). Energy in atomic units

molecular orbital, localized on toluene, to the lowest unoccupied molecular orbital, which is a  $\text{NO}_2^+$  antibonding  $\pi$  orbital ( $|\text{ArH}^+\text{NO}_2\rangle$ ). Mulliken population analysis confirms that the positive charge is wholly localized on  $\text{NO}_2$  in the first region and on toluene in the second one. The first excited singlet state has a parabolic shape, with the minimum located at  $\Theta = 160^\circ$  and  $r = 1.17 \text{ \AA}$ . The minimum energy gap with the ground state is about 4 kcal/mol (Fig. 2).

## 2.2 Diabatic states

As is well known, when two electronic states get close in energy the Born–Oppenheimer approximation breaks down [11] and a correlated treatment of electronic and nuclear motion becomes necessary. This is achieved by simply expanding the total vibronic wavefunction over a set of Born–Oppenheimer functions:

$$\Psi_{\text{tot}} = \sum_{n,v} C_{nv} \psi_{nv}(q, Q) = \sum_{n,v} C_{nv} \phi_n(q, Q) \chi_v(Q), \quad (1)$$

where  $n$  and  $v$  are the electronic and vibrational quantum numbers and  $q$  and  $Q$  denote the electron and nuclear coordinates, respectively. This expansion is always possible because the  $\psi_{nv}$ s form a complete set. The expansion coefficients can be determined by diagonalizing the complete vibronic Hamiltonian, including the terms arising from the nuclear kinetic operator, i.e. those neglected in the Born–Oppenheimer approximation. The latter, though small, are physically significant in as much as they make the Hamiltonian matrix

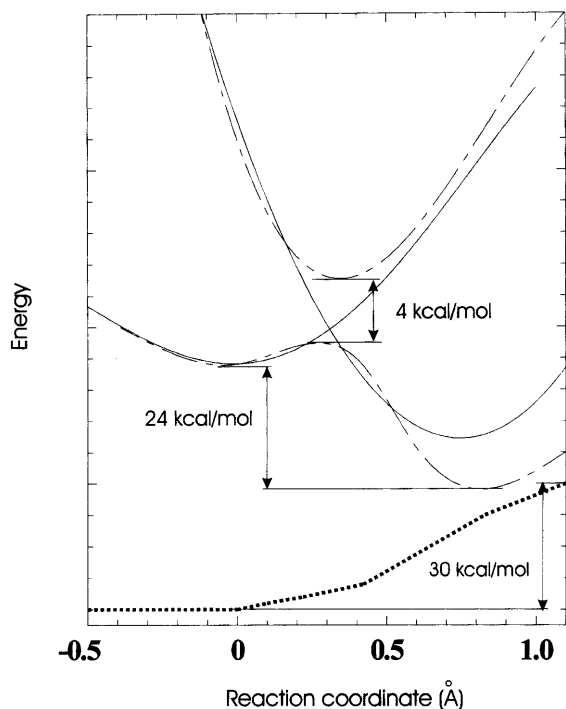


**Fig. 2.** Schematic plot of the adiabatic (*full lines*) and diabatic (*dashed lines*) potential-energy profiles and of the diabatic coupling (*dotted line*) along the minimum energy path for ET. Distances on the path are in angstroms

nondiagonal, determining the transition probabilities between electronic states.

The  $\phi_n$ s can either be chosen as eigenfunctions of the electronic Hamiltonian – adiabatic representation – or as electronic functions whose physical characteristics are preserved throughout the region of the nuclear coordinates of interest – diabatic representation. The adiabatic representation is the most natural, but because of the sudden change in the wave function in the crossing region it involves mathematical difficulties connected with the fact that the nonadiabatic couplings between adiabatic wavefunctions, viz. the first and second derivative of the electronic wavefunctions with respect to the nuclear coordinates, are predicted to diverge in the crossing zones [12]. Diabatic functions do not exhibit abrupt changes in those regions, since they have, by definition, a smooth dependence over the nuclear coordinates. Unfortunately, diabatic states are not uniquely defined. The most natural way to define them, namely that the nuclear kinetic couplings between diabatic functions have to vanish, is revealed to be not a practical one [13]. Thus, one has to resort to defining quasidiabatic electronic functions, for which the nuclear kinetic couplings are small with respect to the electronic couplings.

There are several ways to define quasidiabatic states, all sharing the characteristic that diabatic states are defined via a unitary transformation of the adiabatic ones:

$$|\varphi\rangle = |\phi\rangle U, \quad (2)$$

which allows the high accuracy with which adiabatic states are computed to be extended to the diabatic ones.

The transformation,  $U$ , can be obtained either by minimizing the kinetic couplings between diabatic states, the so-called direct method [14], or by imposing the condition that a suitable property, for example, the dipole moment, of a given electronic state does not change throughout the region of the nuclear coordinates of interest [15]. Excellent reviews can be found in the literature [16]. Here, we preferred to resort to a different method, based on the idea that approximate diabatic states are already intuitively known, and one must find the best transformation to define them in terms of the more accurate adiabatic ones [17]. This method is particularly suitable for ET, since the reference states can be chosen without ambiguity as valence bond configurations with the electron to be transferred localized either on the aromatic substrate or on the nitronium ion. The  $U$  transformation can be found either iteratively [18] or by maximizing the overlap between reference and diabatic states under the orthonormalization condition, using exactly the same procedure already developed to define maximum-overlap atomic hybrids [19, 20].

Let us denote the set of the reference states by  $\{|\zeta\rangle\}$  and let  $\mathbf{S}$  be the overlap matrix between the adiabatic and the reference states:

$$\mathbf{S} = \langle \phi | \zeta \rangle = U^\dagger \langle \phi | \zeta \rangle = U^\dagger \hat{\mathbf{S}} \quad (3)$$

The optimum diabatic states would be those for which the  $\hat{\mathbf{S}}$  matrix is formed by rows containing only one nonzero element, each of which is in different columns. The above condition leads to the eigenvalue equation:

$$\mathbf{S}\mathbf{S}^\dagger U = \lambda^2 U . \quad (4)$$

The eigenvectors  $U_i$ , to which the maximum eigenvalue,  $\lambda_i$ , corresponds will give the optimum expansion of the  $i$ th diabatic state in terms of the adiabatic ones.

The general set of Eq. (4) is not compatible with the condition that the  $U_i$ s are orthogonal to each other. This additional requirement can be accomplished either by using the Schmidt orthogonalization procedure or, following ref. [19], by defining a new transformation  $\hat{U}$ , which satisfies the following requirements: the angles between the  $\hat{U}_i$ s and the  $U_i$ s must be as small as possible and  $\hat{U}_i$ s shall be closer to  $U_i$ s, the higher the eigenvalue  $\lambda_i$ .

It has been shown that the above conditions lead to the equation

$$U\lambda^2 = M\hat{U} , \quad (5)$$

which can be solved by putting  $\hat{U} = \mathbf{V}\mathbf{W}^\dagger$ , where  $\mathbf{V}$  and  $\mathbf{W}$  are unitary matrices which can be obtained by the eigenvalues equations:

$$\lambda^2 U^\dagger U \lambda^2 \mathbf{W} = \mathbf{W} m^2 , \quad (6)$$

$$U \lambda^4 U^\dagger \mathbf{V} = \mathbf{V} m^2 . \quad (7)$$

The energies of the diabatic states and their coupling can then be obtained by projecting the adiabatic Hamiltonian over the diabatic states:

$$\mathcal{H}^{\text{diab}} = \hat{U}^\dagger \epsilon \hat{U} , \quad (8)$$

where  $\epsilon$  is the diagonal matrix of the adiabatic energies.

We applied the above procedure, considering as reference states the antisymmetrized product of the separated reactants, i.e. toluene and  $\text{NO}_2^+$ , and of the separated products, i.e. the toluene cation and the neutral  $\text{NO}_2$ . The lowest ten adiabatic states were considered even though the convergence of Eq. (2) is already satisfactory with the lowest five adiabatic states.

The results are presented schematically in Fig. 2, where the potential-energy profiles of the diabatic states and their coupling, along a path roughly coincident with the minimum energy path of Fig. 1, are reported. It is interesting to note that, in the region of the nuclear configuration of the products,  $|\varphi_2\rangle$  is significantly different from  $|\varphi_1\rangle$ , both for the relative energy and for the minimum position. This is because the minimum energy configuration of the isolated  $\text{NO}_2$  radical is different from that predicted for the  $\text{C}_7\text{H}_8^+-\text{NO}_2$  complex. The minimum of the diabatic state lies at  $\Theta = 137^\circ$ ,  $r = 1.19$  Å. For the same reason the coupling between  $|\varphi_1\rangle$  and  $|\varphi_2\rangle$  is also large in this region.

### 2.3 Vibrational states and transition probabilities

The vibrational states of the two crossing diabatic states were computed variationally, using two sets of product harmonic wave functions centered on the minima of each diabatic state:

$$\chi_i^{\text{tot}}(R, \Theta) = \chi_{\text{si}}(R - R_i^0) \chi_{\text{bi}}(\Theta - \Theta_i^0) . \quad (9)$$

The Hamiltonian matrix elements were evaluated by Hermite numerical integration, using a two-dimensional

spline interpolation of a grid of the potential energy and coupling surfaces. For  $|\varphi_1\rangle$  the computed frequencies are  $750$   $\text{cm}^{-1}$  for the bending mode and  $1520$   $\text{cm}^{-1}$  for the symmetric stretching; the experimental values for isolated  $\text{NO}_2^+$  are  $639$  and  $1397$   $\text{cm}^{-1}$ , respectively [21]. For  $|\varphi_2\rangle$  the computed vibrational frequencies are  $1000$  and  $1640$   $\text{cm}^{-1}$  for the bending and the symmetrical stretching, respectively, the experimental values for the isolated  $\text{NO}_2$  radical being  $750$  and  $1361$   $\text{cm}^{-1}$ , respectively [22]. There is a certain discrepancy between computed and observed frequencies. Of course, the observed frequencies refer to isolated  $\text{NO}_2^+$  and  $\text{NO}_2$ , whereas the computed ones refer to the whole complex, but it is probable that the computed values are overestimated both because correlation effects are not fully accounted for and because of the limited number of states used in the diabaticization process, especially in the region where  $\varphi_2$  becomes the ground state. In fact, for the minimum at  $\Theta = 132^\circ$ ,  $r = 1.21$  Å, the adiabatic potential-energy surface yields  $1052$  and  $1492$   $\text{cm}^{-1}$  for the bending and the symmetric stretching, respectively. It is noteworthy that after diagonalization of the total Hamiltonian, including electronic coupling, the ground vibrational state of the  $\pi$  complex is located around  $\Theta = 132^\circ$ , as the ground vibrational state of the adiabatic potential-energy surface.

Next, we evaluated the Born probabilities for ET, by assuming that the system was initially prepared in the Boltzmann distribution at  $298$  K of the set  $|\chi_1\rangle$  and by summing over all  $|\chi_2\rangle$  states. The results are reported in Fig. 3.

After  $200$  fs the probability that the vibrational states of  $|\chi_2\rangle$  are populated is about  $0.12$ . Now, since ET is highly exergonic, it is reasonable to assume that the fraction of molecules found in any of the  $|\chi_2\rangle$  states will be trapped there by fast decay into lower energy vibrational states. Thus after a few tens of the transition period all molecules will be found in the  $|\chi_2\rangle$  states, namely the ET states. That means that ET is a very fast process, occurring on a timescale of a few picoseconds. This is not surprising in view of the low effective mass of the bending mode [23], which makes tunneling very important, and of the modest displacement of the two diabatic states along the symmetrical stretching coordinate.

To test the reliability of the results, we also carried out the computation of the transition probabilities by representing the two diabatic states by two parabolic functions, with the harmonic frequencies taken to be equal to those observed for isolated  $\text{NO}_2^+$  and  $\text{NO}_2$ , and using the computed relative energy and coupling of Fig. 2. The results are reported in Fig. 3. The transition time does not change significantly, whereas the transition probability rises, because of the higher density of states of the product well around the crossing point, due to the fact that the experimental frequencies of  $\text{NO}_2$  are significantly lower than the calculated ones.

### 3 Concluding remarks

The results of the present dynamical study have important implications for the mechanism of aromatic nitration. In fact, they show that ET from the aromatic

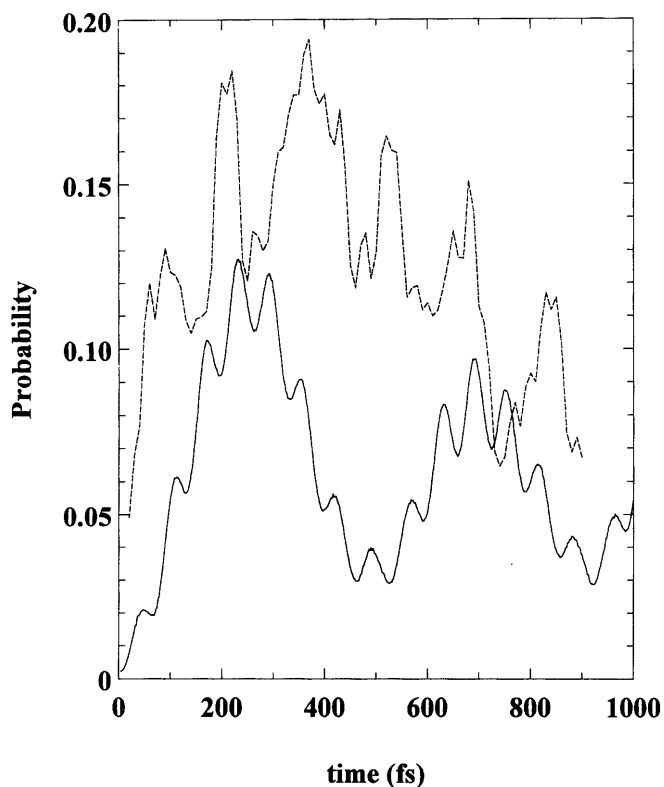


**Fig. 3.** ET probability as a function of time. The *full line* refers to values obtained using the computed energies and shapes of the diabatic state; the *dotted line* refers to ET probabilities from the harmonic model employing the computed relative energy and diabatic coupling and the experimental frequencies of isolated  $\text{NO}_2^+$  and the  $\text{NO}_2$  radical

substrate to the nitronium ion is very fast and this would imply that during the approach of the nitronium ion to the aromatic substrate there is a high probability that ET from the aromatic substrate to nitronium ion occurs.

The paradox of the high positional selectivity without substrate selectivity is removed: the attacking species is no longer the nitronium ion, which reacts with all aromatics at encounter-limited rates, but the radical  $\text{NO}_2$ . The latter is compatible with the observed positional selectivity, since the radical-pair recombination is spin-density driven.

The present results also hint at a possible mechanistic explanation of the fact that nitration rates are encounter-limited for almost all aromatics. In fact, if ET occurs each time the two reactants are in the same solvation shell, each collision will lead to nitration products, since the dissociation of the radical pair will be a highly endoergonic process, both because ET is highly exergonic, about 1 eV for toluene, and because the higher solvation energy of the smaller nitronium ion with respect to the aromatic radical cation makes the dissociation of the radical pair difficult. Thus, aromatic nitration could be a case where a harpoon-type mechanism applies [25]. In

contrast to the reaction of  $\text{I}_2$  with K, where the transfer of an electron from iodine to K provides the attractive force which keeps the two reactants together, here the force is provided by the fact that in solution the dissociation of the radical pair appears to require a significant energy barrier.

*Acknowledgement.* The financial support of the Italian CNR is gratefully acknowledged.

## References

- (a) Ingold CK (1969) Structure and mechanism in organic chemistry, 2nd edn. Cornell University Press, Ithaca; (b) Schoefied K (1980) Aromatic nitration. Cambridge University Press, Cambridge
- (a) Olah GA (1971) *Acc Chem Res* 4: 240; (b) Moodie RB, Schoefied K, Weston JB (1974) *J Chem Soc Chem Commun* 382
- Ridd JH (1971) *Acc Chem Res* 4: 248
- Perrin CL (1977) *J Am Chem Soc* 99: 550
- (a) Hückel E (1936) *Z Phys Chem Abt B* 35: 136; (b) Weiss J (1933) *Trans Faraday Soc* 42: 116; (c) Kenner J (1945) *Nature* 156: 369; (d) Pedersen EB, Petersen TE, Torssell K, Lawesson SO (1973) *Tetrahedron* 29: 579
- Benford GA, Benton CA, Halberstadt ES, Hughes ED, Ingold CK, Minkoff GJ, Reed RI (1945) *Nature* 156: 688
- Eberson L, Radner F (1987) *Acc Chem Res* 20: 53
- Peluso A, Del Re G (1996) *J Phys Chem* 100: 5303
- Szabó KJ, Hörnfeldt A, Gronowitz S (1992) *J Am Chem Soc* 114: 6287
- Schmidt MW, Baldrige KK, Boatz JA, Elbert ST, Gordon MS, Jemsen JJ, Koseki S, Matsunaga M, Nguyen KA, Su S, Windus TL, Dupuis M, Montgomery JA (1993) *J Comput Chem* 14: 1347
- (a) Herzberg G, Longuet-Higgins HC (1963) *Discuss Faraday Soc* 35: 77; (b) Peluso A, Santoro F, Del Re G (1996) *Int J Quantum Chem* 63: 233
- Teller E (1937) *J Phys Chem* 41: 109
- Mead CA, Truhlar DG (1979) *J Chem Phys* 70: 2284
- Desouter-Lecomte M, Ley-Nihant B, Praet MT, Lorquet JC (1987) *J Chem Phys* 86: 1429
- Macias A, Riera A (1978) *J Phys B* 11: L849
- (a) Sidis V (1992) *Adv Chem Phys* 82: 73; (b) Lengsfeld III BH, Yarkony DR (1992) *Adv Chem Phys* 82: 1; (c) Durand P, Malrieu JP (1987) *Adv Chem Phys* 67: 321; (d) Cimraglia R, Malrieu JP, Persico M, Spioegelmann F (1985) *J Phys B At Mol Opt Phys* 18: 3073
- (a) Levy B (1981) In: Wende B (ed) *Spectral line shape*. de Gruyter, Berlin, p 165; (b) Levy B (1981) In: Carbo R (ed) *Current aspects of quantum chemistry*. Elsevier, Amsterdam, p 127
- Persico M (1985) *Spectral Line Shapes* 3: 21
- Del Re G (1963) *Theor Chim Acta* 1: 188
- Petsalakis ID, Theodorakopoulos G, Nicolaidis CA, Buenker RJ (1991) *Chem Phys Lett* 185: 359
- Bryant G, Jiang Y, Grant E (1992) *Chem Phys Lett* 200: 495
- Arakawa ET, Nielsen AH (1958) *J Mol Spectrosc* 2: 413
- Wilson Jr EB, Decius JC, Cross PC (1955) *Molecular vibrations*. McGraw-Hill, New York
- Peluso A, Brahim M, Carotenuto M, Del Re G (1998) *J Phys Chem* 102: 10333
- Herschbach DR (1966) *Adv Chem Phys* 10: 319